


Article

Synthesis and Structural Characterization of Amidine, Amide, Urea and Isocyanate Derivatives of the Amino-*closo*-dodecaborate Anion $[B_{12}H_{11}NH_3]^-$

Yuanbin Zhang ^{1,2,†}, Yuji Sun ^{1,†}, Tao Wang ¹, Jiyong Liu ¹, Bernhard Spingler ³  and Simon Duttwyler ^{1,*}

¹ Department of Chemistry, Zhejiang University, 38 Zheda Road, Hangzhou 310027, China; 15868145065@126.com (Y.Z.); sunyuji1991@163.com (Y.S.); 21637046@zju.edu.cn (T.W.); liujiyong1205@163.com (J.L.)

² Key Laboratory of Biomass Chemical Engineering of Ministry of Education, Department of Chemical and Biological Engineering, Zhejiang University, 38 Zheda Road, Hangzhou 310027, China

³ Department of Chemistry, University of Zurich, Winterthurerstrasse 190, 8057 Zurich, Switzerland; spingler@chem.uzh.ch

* Correspondence: duttwyler@zju.edu.cn

† These authors contributed equally to this work.

Received: 1 November 2018; Accepted: 16 November 2018; Published: 29 November 2018



Abstract: The synthesis and structural characterization of new derivatives of $[B_{12}H_{12}]^{2-}$ is of fundamental interest and is expected to allow for extended applications. Herein we report on the synthesis of a series of amidine, amide, urea and isocyanate derivatives based on the amino-*closo*-dodecaborate anion $[B_{12}H_{11}NH_3]^-$. Their structures have been confirmed by spectroscopic methods, and nine crystal structures are presented.

Keywords: dodecaborate; boron cluster; borane; amidine; amide; urea; isocyanate

1. Introduction

The *closo*-dodecaborate dianion $[B_{12}H_{12}]^{2-}$ (**1**, Figure 1) is an icosahedral boron cluster with 12 identical B–H vertices, and it possesses unique properties such as spherical electron delocalization and high thermal/chemical stability [1–4]. It is considered a 3D analogue of benzene, and applications of $[B_{12}H_{12}]^{2-}$ as well as its derivatives have been found in many fields, such as weakly coordinating anions [5–14], medicinal chemistry [15–17], catalysis [18,19], ligand design [20–22] and supramolecular chemistry [23–27].

Since the isolation of **1** in 1960 [28], many routes to substituted *closo*-dodecaborate anions have been reported *via* the construction of B–N, B–O, B–S, B–Hal or B–C bonds [29], and the ammonium dodecaborate $[B_{12}H_{11}NH_3]^-$ (**2**) serves as one of the fundamental building blocks for further functionalization [30]. Monoanionic **2** can be synthesized from the reaction of **1** with hydroxylamine-*O*-sulfonic acid (H_2N-SO_3H) on a multi-gram scale [30–32]. The $-NH_3$ site can be deprotonated under basic conditions and then combined with acyl chlorides, carbodiimides or aldehydes to afford the corresponding amides **3** [33–37], guanidines **4** [34] and imines **5** [38]. Dodecaborate amidines **6** have not been explored yet, and urea derivatives **7** were unknown until we recently found that the reaction of **2** with dialkylcarbamoyl chlorides $ClC(O)NMe_2$ or $ClC(O)NEt_2$ affords the corresponding $\{B_{12}\}$ -substituted *N,N*-dialkyl ureas [39]. The isocyanate derivative **8** was originally synthesized from the reaction of the carbonyl derivative $[B_{12}H_{11}(CO)]^-$ with NaN_3 but characterized only by ^{11}B -NMR and IR spectroscopy [40]. Herein we present: (1) the synthesis of three new $\{B_{12}\}$ -based amidines **6** with two crystal structures; (2) six crystal structures of $\{B_{12}\}$ -based

amides **3** and a simple approach for the interconversion between their dianionic and monoanionic forms; (3) the synthesis of two new $\{B_{12}\}$ -based aromatic ureas **7**; (4) a new route to isocyanate **8** and its crystal structure.

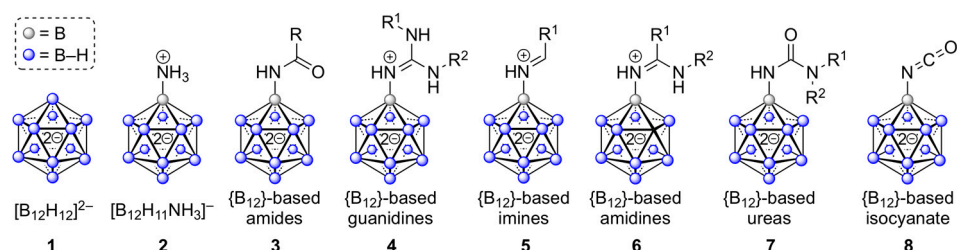
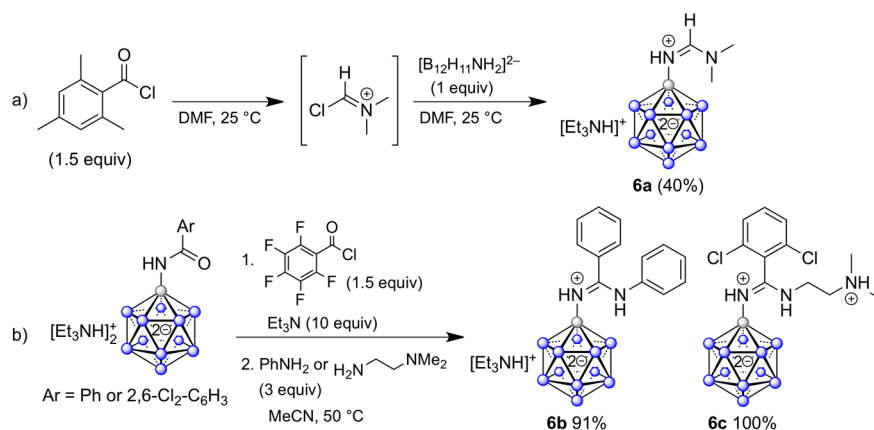


Figure 1. General structures of the parent *closo*-dodecaborate dianion $[B_{12}H_{12}]^{2-}$ and its derivatives.

2. Results and Discussion

2.1. Synthesis of $\{B_{12}\}$ -based Amidinium Ions

Amidine derivatives based on the $\{B_{12}\}$ cluster have not been reported before, and in the following, methods to synthesize them are presented. Combination of dimethyl formamide with 2,4,6-trimethylbenzoyl chloride afforded the chloroiminium intermediate, which upon attack by $[B_{12}H_{11}NH_2]^{2-}$ afforded **6a** (Scheme 1a). This reaction allowed for the isolation of the desired product; however, the yield of 40% was moderate, and furthermore extension of the substrate scope by this method did not appear convenient. Using a related strategy, we found that the carbonyl group of $\{B_{12}\}$ -based amides can be activated by pentafluorobenzoyl chloride, and subsequent attack by amines would then lead to $\{B_{12}\}$ -based amidinium ions (Scheme 1b). Following this approach, products **6b** and **6c** were isolated in excellent yields of 91% and 100%, respectively.



Scheme 1. Synthesis of $\{B_{12}\}$ -based amidinium ions **6a–c** using (a) the chloroiminium intermediate derived from dimethylformamide and (b) pentafluorophenylbenzoyl chloride as activating agent.

Single crystals of **6a** and **6c** were obtained from acetonitrile solutions, and ORTEP representations of **6a** and **6c** are displayed in Figure 2. Observed distances (Å) are B1–N1 1.520(2), N1–C1 1.3078(18), C1–N2 1.3092(19), N2–C2 1.451(2) and N2–C3 1.4662(19) for **6a**; B1–N1 1.534(4), N1–C1 1.312(4), C1–N2 1.331(4), C1–C2 1.485(4) and N2–C8 1.420(4) for **6b**. These structural features are similar to those of typical organic amidinium ions; in addition, the coordination geometry around C1 is perfectly trigonal-planar for both products with a sum of angles of 360° . The torsion angles N1–C1–N2–C2 and N1–C1–N2–C3 of **6a** are $0.0(2)$ and $-175.35(15)^\circ$, respectively, indicating coplanarity of the amidine and the dimethylamino moieties. On the other hand, **6b** is more twisted with a torsion angle N1–C1–N2–C8 of $154.4(3)^\circ$.

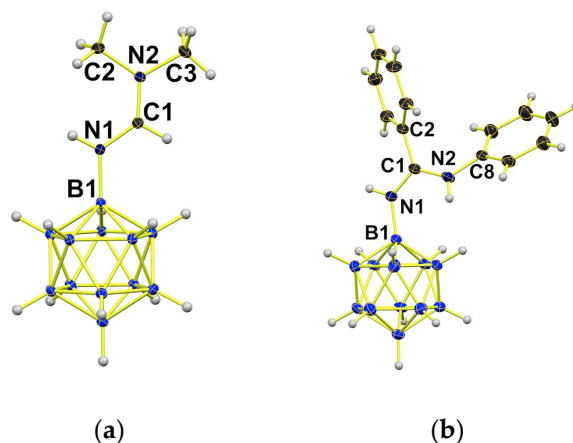
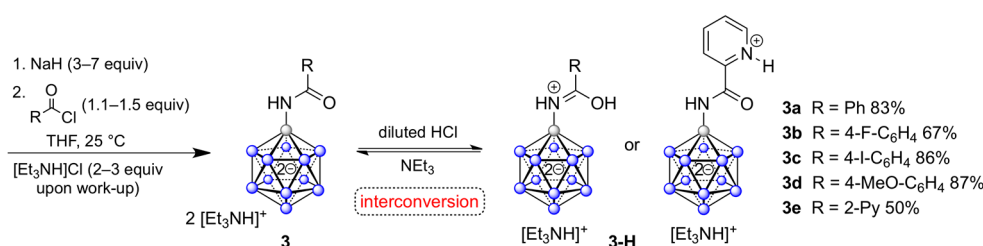


Figure 2. Crystal structures of (a) **6a** and (b) **6b**; cations and solvent molecules are omitted for clarity, and thermal ellipsoids are displayed at the 30% level.

2.2. Synthesis of $\{B_{12}\}$ -based Amides

$\{B_{12}\}$ -based amides **3** were originally synthesized by other groups [33–36]. The products were isolated in their *O*-protonated form **3-H**, and there was only one crystal structure reported, namely **3a-H** with R = Ph (Scheme 2). Our group recently modified the reaction conditions, and the products were obtained in up to 95% yields in the *O*-deprotonated form **3** after chromatography on silica gel [36]. Our approach uses smaller amounts of acyl chlorides and a slight excess of sodium hydride base, which results in the isolation of the dianionic form (for this study, **3a–d** were resynthesized according to [37] in order to probe their solid-state structures). Adjustment of the pH value with diluted hydrochloric acid during the work-up or after isolation leads to **3-H** in their *O*-protonated form. Back-conversion to **3** can be achieved by dissolution in MeCN, treatment with Et₃N and distillation of all the volatiles. Pyridine-substituted **3e** was synthesized as a new product. Since purification by chromatography proved difficult, it was isolated as **3e-H** in 50% yield upon acidic work-up and recrystallization from methanol. Conversion to **3e** occurred quantitatively using the above-mentioned procedure. In contrast to previously described amides, protonation of **3e** takes place at the pyridine ring, indicating the higher basicity of the heterocycle as compared to the amide moiety. The ¹¹B{¹H}-NMR spectra of **3b**, **3b-H**, **3e** and **3e-H** are shown in Figure S1 as representative examples to demonstrate the effect of protonation. For R = Ph (**3a**), 4-F-C₆H₄ (**3b**), 4-I-C₆H₄ (**3c**), 4-MeO-C₆H₄ (**3d-H**), 2-pyridyl (**3e**) and 2-pyridyl-H (**3e-H**), crystal structures were elucidated, and selected structural features are discussed below.



Scheme 2. Synthesis of $\{B_{12}\}$ -based amides **3** and interconversion between their dianionic and monoanionic forms; compounds **3a–d** were prepared according to [37].

Single crystals of **3a**, **3b**, **3c**, **3d-h**, **3e** and **3e-H** were obtained from acetonitrile, acetone, acetonitrile-acetone or acetonitrile-methanol solutions. ORTEP representations are displayed in Figure 3, and a summary of structural parameters is given in Table 1, including data for *O*-protonated **3a-H**, originally reported by Gabel and coworkers [34]. The seven compounds can be grouped into the series **3a/3b/3c/3e/3e-H** and **3a-H/3d-H**. For the former series, distances (Å) fall within B1–N1 1.51–1.52, N1–C1 1.31–1.33 and C1–O1 1.23–1.25. These compounds thus exhibit strong structural resemblance to classical organic amides. For the latter pair, observed ranges (Å) are B1–N1 1.53–1.58,

N1–C1 1.26–1.30 and C1–O1 1.31–1.34. These values are consistent with O-protonation, leading to a more pronounced allyl cation-type equalization of bond lengths. On the other hand, all seven products share two features: The central carbon atom C1 has perfect trigonal-planar geometry with a sum of angles of 360° . Furthermore, the torsion angles O1–C1–C2–C3 (O1–C1–C2–N2 for **3e-H**) fall in the range of -18° to $+32^\circ$ and indicate a certain degree of conjugation between the aromatic rings and the N1–C1–O1 π system.

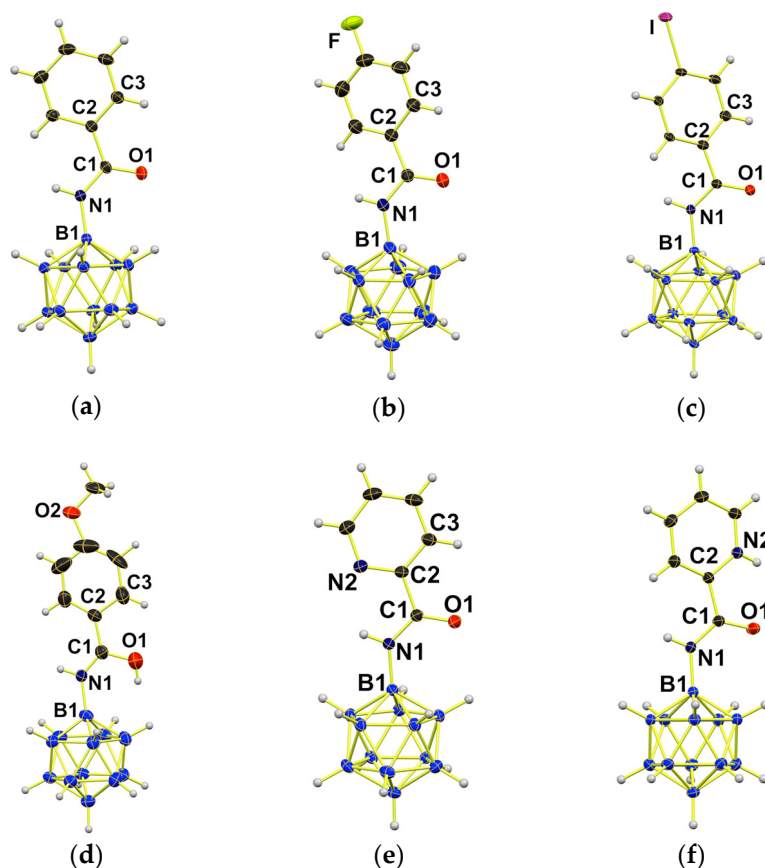


Figure 3. Crystal structures of (a) **3a**, (b) **3b**, (c) **3c**, (d) **3d-H**, (e) **3e** and (f) **3e-H**; cations and solvent molecules are omitted for clarity, and thermal ellipsoids are displayed at the 30% level.

Table 1. Selected bond lengths and angles for **3a**, **3a-H**, **3b**, **3c**, **3d-H**, **3e** and **3e-H**.

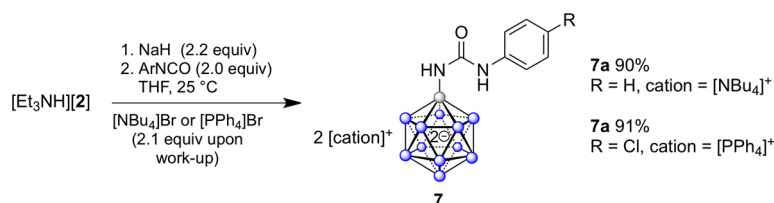
Distance [Å]/Angle [°]	3a ¹	3a-H ²	3b	3c	3d-H	3e	3e-H
B1–N1	1.520(6)	1.534(4)	1.516(4)	1.512(5)	1.577(7)	1.516(3)	1.524(3)
N1–C1	1.324(6)	1.295(7)	1.320(4)	1.327(4)	1.263(7)	1.306(2)	1.316(3)
C1–O1	1.250(5)	1.314(2)	1.238(3)	1.227(4)	1.343(8)	1.234(2)	1.232(3)
C1–C2	1.496(6)	1.471(2)	1.500(4)	1.500(5)	1.466(17)	1.502(3)	1.512(3)
Σ (C1)	359.9	359.9	360.0	360.0	359.9	360.0	360.0
O1–C1–C2–C3 ³	−17.8(3)	−9.95(13)	−15.6(4)	32.0(3)	−4.9(4)	5.77(2)	7.4(3)

¹ Parameters of one of the two molecules in the asymmetric unit; ² data from reference [34]; ³ torsion angle O1–C1–C2–N2 for **3e-H**.

2.3. Synthesis of $\{B_{12}\}$ -based Ureas

$\{B_{12}\}$ -based ureas with $N\{B_{12}\}, N'$ (aryl) substitution have not been reported before. The synthetic strategy to prepare dodecaboranyl N, N' -dialkyl ureas recently reported by our group involved the combination of **2** with dialkylcarbamoyl chlorides [39]. We wondered whether aromatic isocyanates could be used instead of carbamoyl chlorides to achieve the new substitution pattern, given the

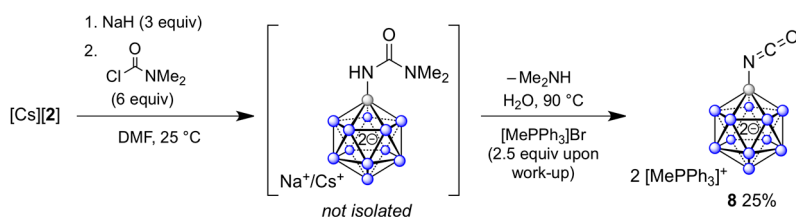
commercial availability of many ArNCO reagents. We found that the reaction of **2** with aromatic isocyanates under basic conditions directly leads to the formation of the corresponding urea derivatives of the structure $\{B_{12}\}NH-C(O)-NHAr$. Thus, the transformations with commercially available PhNCO and 4-Cl-C₆H₄NCO cleanly gave products **7a** and **7b** in yields of 90% and 91% (Scheme 3). They were isolated by precipitation upon cation exchange to $[NBu_4]^+$ or $[PPh_4]^+$ and characterized by NMR spectroscopy and mass spectrometry.



Scheme 3. Synthesis of $\{B_{12}\}$ -based ureas **7**.

2.4. Synthesis of Dodecaboranyl Isocyanate

Isocyanates are important intermediates in organic synthesis that are used in the manufacture of, e.g., agrochemicals and polyurethanes [41]. Only one publication by Alam and coworkers from 1989 mentioned the isolation of dodecaboranyl isocyanate **8** [40]. It was prepared *via* the reaction of $[B_{12}H_{11}(CO)]^-$ with NaN_3 and analyzed by ¹¹B-NMR and IR spectroscopy. However, further characterization was not given, and in particular the crystal structure was not reported. Because the isocyanate moiety serves as versatile functional group handle capable of providing access to a number of novel $\{B_{12}\}$ -based derivatives, we were interested in resynthesizing **8**. However, multiple attempts to reproduce the original procedure were not successful in our laboratory, and we therefore sought to establish an alternative route. Since dodecaboranyl *N,N*-dialkyl ureas can be prepared easily [39], their thermal fragmentation appeared as an attractive strategy. Indeed, treatment of **2** with base and $ClC(O)NMe_2$ to give the intermediate urea, followed by heating in water, afforded **8** in 25% overall yield (Scheme 4). The yield of this sequence is rather low, and efforts to improve the protocol are ongoing.



Scheme 4. Synthesis of isocyanate **8**.

In acetonitrile-*d*₃ solution, the ¹¹B NMR shifts of **8** were -7.7 , -15.4 , -16.7 and -19.3 ppm, while ¹H NMR resonances appeared at 1.23, 0.97 and 0.75 ppm. The NCO ¹³C NMR signal could not be detected unambiguously; it is known from organic isocyanates that this signal can be very broad and difficult to observe. Interestingly, **8** is inert towards air and moisture. Solutions in acetone, kept under ambient conditions, remained unchanged over six months. The IR spectrum showed characteristic absorptions at 2479 cm^{-1} , 2308 cm^{-1} and 1438 cm^{-1} stemming from B–H, $\nu_{\text{asymmetric}}(\text{NCO})$ and $\nu_{\text{symmetric}}(\text{NCO})$ stretchings, respectively (Figure 4a) [42].

Colorless single crystals of **8** were obtained from acetone solution. X-Ray diffraction revealed distances (Å) of B1–N1 1.499(3), N1–C1 1.138(3) and C1–O1 1.186(3), clearly indicating the two double bonds of the N=C=O moiety (Figure 4b). This finding is in agreement with the angle N1–C1–O1 of $176.5(3)^\circ$, showing almost linear geometry of the isocyanate group. The B1–N1–C1 angle of $163.1(3)^\circ$ is also quite large, while no unusual structural features were observed for the $\{B_{12}\}$ cluster.

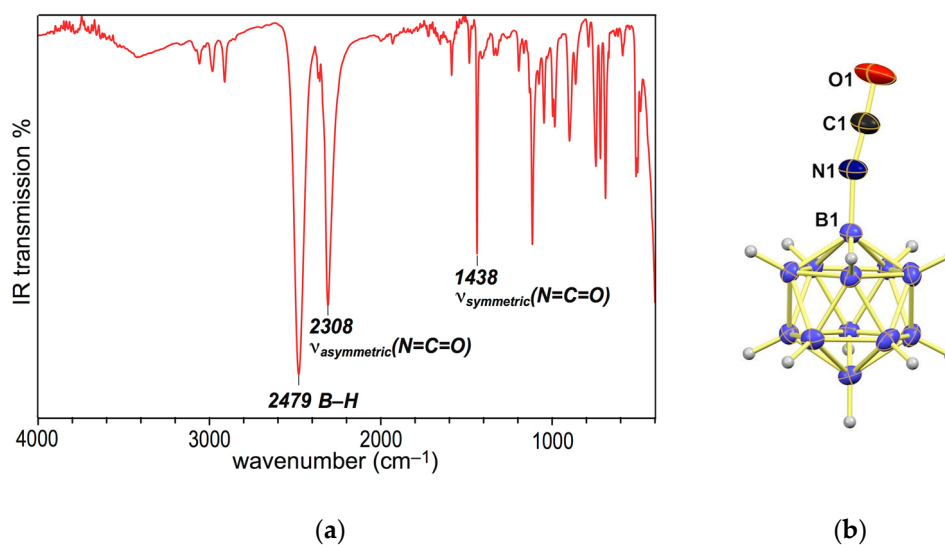


Figure 4. (a) IR spectrum and (b) crystal structure of [MePPh₃]₂[B₁₂H₁₁NCO]; cations in the crystal structure omitted for clarity, thermal ellipsoids displayed at the 30 % level.

3. Materials and Methods

3.1. General

If not otherwise specified, reagents and organic solvents were commercially available and used without further purification. Anhydrous solvents were prepared by passage through activated Al₂O₃ and stored over 3 Å molecular sieves. CD₃CN and CD₂Cl₂ were purchased from Cambridge Isotope Laboratories and filtered through Al₂O₃ prior to use. [B₁₂H₁₂]²⁻ and [B₁₂H₁₁NH₃]⁻ salts and dodecaborate amides **3a–e** were prepared according to the literature [10,36].

Glassware for air-sensitive reactions was dried at 150 °C and allowed to cool in a vacuum. Reactions carried out in a glovebox were run under a nitrogen atmosphere with O₂, H₂O < 1 ppm.

Thin-layer chromatography (TLC) was carried out using silica gel 60, F254 with a thickness of 0.25 mm. Column chromatography was performed on silica gel 60 (200–300 mesh).

Low-resolution ESI-MS data were recorded on Advion Expression CMS instrument (Advion, Ithaca, NY, USA). High-resolution MS data were recorded using IT-TOF detection (Shimadzu, Kyoto, Japan) equipped with an electrospray ionization source (ESI). Accurate mass determination was corrected by calibration using sodium trifluoroacetate clusters as a reference.

Single-crystal X-ray diffraction studies were performed on an Oxford Diffraction Gemini A Ultra diffractometer (Agilent Technologies, Santa Clara, CA, USA) equipped with an 135 mm Atlas CCD detector and using Mo K-α radiation.

NMR spectra were recorded on a Bruker AVANCE III 500 spectrometer (¹H NMR 500.13 MHz, ¹³C NMR 125.77 MHz, ¹¹B NMR 160.46 MHz) or a Bruker AVANCE III 400 spectrometer (Bruker, Billerica, MA, USA) (¹H NMR 400.13 MHz, ¹³C NMR 100.62 MHz, ¹¹B NMR 128.38 MHz) at the temperature indicated. Data are reported as follows: Chemical shift in ppm, multiplicity (s = singlet, d = doublet, t = triplet, q = quartet, m = multiplet, dd = doublet of doublets, etc.), coupling constant *J* in Hz, integration, and (where applicable) interpretation. Signals were referenced against solvent peaks (¹H: residual CHD₂C(O)CD₃ = 2.05 ppm, residual CHD₂CN = 1.94 ppm, residual CHDCl₂ = 5.32 ppm, ¹³C{¹H}: CD₃C(O)CD₃ = 29.84 ppm, CD₃CN = 1.32 ppm, CD₂Cl₂ = 53.32 ppm). ¹¹B and ¹¹B{¹H} NMR spectra were calibrated against external BF₃·Et₂O = 0 ppm (BF₃·Et₂O capillary in C₆D₆).

3.2. Experimental Section

Synthesis of [Et₃NH](3e-H): In a glovebox filled with N₂, a 20 mL vial was charged with [Et₃NH][B₁₂H₁₁NH₃] (212.4 mg, 0.817 mmol, 1 equiv), NaH (138.2 mg, 5.758 mmol, 7 equiv) and a stir

bar. THF (4 mL) and DMF (4 mL) were added, and the mixture was stirred at room temperature for 10 min until there was no H₂ evolution anymore. Then pyridine-2-carbonyl chloride hydrochloride PyCOCl·HCl (220.2 mg, 1.237 mmol, 1.5 equiv) was slowly added. The conversion was complete after stirring for 5 h. The flask was transferred out of the glovebox. H₂O (4 mL) was added, and the pH value of the reaction mixture was adjusted to 2–3 with 1 M aqueous HCl. [NEt₃H]Cl (300 mg, 2.180 mmol, 2.7 equiv) was added, and the reaction mixture was extracted with MeCN/EtOAc (1:2 v/v). The organic layers were concentrated on a rotary evaporator. The residue was purified by recrystallization from methanol to afford yellowish crystals of [Et₃NH][**3e-H**] (150 mg, 50%). ¹H{¹¹B} NMR (400 MHz, CD₃CN): δ = 8.96 (s, 1H, anionic NH), 8.90–8.86 (m, 1H, Py H), 8.18–8.14 (overlapping m, 2H, Py H), 7.89–7.72 (m, 1H, Py H), 6.63 (t, 1H, J_{NH} = 52 Hz, NH), 3.27 (s, 1H, NH), 3.20–3.15 (m, 6H, cationic N–CH₂), 1.47 (broad signal, 5H, B–H), 1.24 (t, J = 7.4 Hz, 9H, cationic CH₃), 1.20 (broad signal, 5H, B–H), 1.13 (broad signal, 1H, B–H). ¹³C{¹H} NMR (101 MHz, CD₃CN): δ = 166.7, 149.5, 143.9, 141.5, 129.8, 124.5 (6 anionic signals), 48.0, 9.2 (2 cationic signals). ¹¹B{¹H} NMR (128 MHz, CD₃CN): δ = –7.6 (1B, B–N), –15.3 (5B, B–H), –15.7 (overlapping signals, 6B, B–H). High-resolution ESI-MS (negative mode, MeOH): *m/z* calcd for [C₆H₁₇B₁₂N₂O][–] 263.2430. Found: 263.2459.

Transformation of [Et₃NH](3e-H) to [Et₃NH]₂(3e): A 20 mL vial was charged with [Et₃NH][**3e-H**] (50 mg) and a stir bar. MeCN (3 mL) and Et₃N (0.5 mL) were added, and the solution was stirred at room temperature for 1 h. Then the stir bar was removed, and the solution was concentrated on a rotary evaporator and dried overnight under vacuum at 80 °C to afford compound [Et₃NH]₂[**3e**] in quantitative yield. This method can also be applied for the transformation of other compounds **3-H** to **3** quantitatively. ¹¹B{¹H} NMR spectra of **3b**, **3b-H**, **3e** and **3e-H** are displayed in Figure S1. ¹H{¹¹B} NMR (400 MHz, CD₃CN): δ = 8.56 (broad signal, 1H, Py H), 8.09–8.00 (m, 1H, Py H), 7.99–7.80 (overlapping m, 2H, Py H and amide N–H), 7.50–7.38 (m, 1H, Py H), 4.63 (broad t, 2H, J_{NH} = 52 Hz, N–H from cation), 3.25–3.01 (m, 12H, cationic N–CH₂), 1.34 (s, 5H, B–H), 1.24 (t, J = 7.4 Hz, 9H, cationic CH₃), 1.03 (broad signal, 5H, B–H), 0.89 (broad signal, 1H, B–H). ¹³C{¹H} NMR (101 MHz, CD₃CN): δ = 166.2, 152.9, 149.0, 138.5, 126.4, 122.2 (6 anionic signals), 47.8, 9.1 (2 cationic signals). ¹¹B{¹H} NMR (128 MHz, CD₃CN): δ = –5.3 (1B, B–N), –15.3 (5B, B–H), –16.4 (5B, B–H), –18.7 (1B, B–H). High-resolution ESI-MS (negative mode, MeOH): *m/z* calcd for [C₆H₁₇B₁₂N₂O]^{2–} 131.1226. Found: 131.1254.

Synthesis of amidine [Et₃NH](6a): In a glovebox, a dry 20 mL vial, equipped with a stir bar, was charged with [Et₃NH][B₁₂H₁₁NH₃] (102 mg, 0.40 mmol, 1 equiv). Then anhydrous DMF (1 mL) was added. The vial was transferred to a fumehood, and dry Et₃N (1.0 mL, 7.20 mmol, 18 equiv) was added to the solution under N₂ protection. Then 2,4,6-trimethylphenylcarboxylic acid chloride (110 mg, 0.60 mmol, 1.5 equiv) was added. The mixture was stirred at 25 °C for 4 h. The reaction was quenched with an aqueous [Et₃NH]Cl solution (2 mL H₂O + 2 equiv [Et₃NH]Cl); the pH value at this point was ca. 7–8. The mixture was extracted with DCM/MeCN = 4: 1 (8 × 10 mL). The combined organic layers were dried over MgSO₄, and the solution was filtered and concentrated by rotary evaporation. The cloudy residue was purified by silica gel column chromatography (eluent DCM/MeCN = 10:3, fraction size 20 mL). The combined eluates were concentrated on a rotary evaporator and dried under vacuum at 60 °C overnight to afford compound [Et₃NH][**6a**] as a colorless solid (50.4 mg, 40%). ¹H{¹¹B} NMR (400 MHz, CD₃CN, 23 °C): δ 7.76 (d, J = 16.0 Hz, 1H, N=CH–N), 6.41 (broad signal, 1H, N–H), 3.13 (q, J = 7.2 Hz, 6H, cationic N–CH₂), 3.08 (s, 3H, anionic N–CH₃), 2.83 (s, 3H, anionic N–CH₃), 1.26 (broad signal, 5H, B–H), 1.24 (t, J = 7.2 Hz, 9H, cationic N–CH₂CH₃), 1.03 (broad signal, 5H, B–H), 0.85 (broad signal, 1H, B–H). ¹³C{¹H} NMR (100 MHz, CD₃CN, 23 °C): δ 157.3 (N=C–N), 48.0 (cationic CH₂), 43.1, 35.7 (two N–C signals), 9.2 (cationic CH₃). ¹¹B{¹H} NMR (160 MHz, CD₃CN, 23 °C): δ –4.2 (1B, B–N), –14.5 to –17.0 (10B, B–H), –19.0 (1B, B–H). High-resolution ESI-MS (negative mode, MeOH): *m/z* calcd for [C₃H₁₉B₁₂N₂][–]: 213.2738. Found: 213.2762.

Synthesis of amidine [Et₃NH](6b): A dry 20 mL vial, equipped with a stir bar, was charged with [Et₃NH]₂[B₁₂H₁₁NHCOC₆H₅] (101 mg, 0.22 mmol, 1 equiv). Then anhydrous MeCN (3 mL) was added, and dry Et₃N (0.3 mL, 2.16 mmol, 9.8 equiv) was added to the solution under N₂ protection.

Pentafluorophenylcarboxylic acid chloride (80.0 mg, 0.35 mmol, 1.5 equiv) was added at 25 °C. The temperature was raised to 50 °C. After 30 min, aniline (61 mg, 0.66 mmol, 3.0 equiv) was added. The mixture was stirred for another 4 h and concentrated by rotary evaporation. The cloudy residue was purified by silica gel column chromatography (eluent DCM/MeCN = 4:1, fraction size 20 mL). The combined eluates were concentrated on a rotary evaporator and dried under vacuum at 60 °C overnight to afford compound [Et₃NH][6b] as a yellow solid (87.7 mg, 91%). ¹H{¹¹B} NMR (400 MHz, CD₂Cl₂, 23 °C): δ 10.00 (s, 1H, N–H), 7.53–7.48 (m, 1H, phenyl H), 7.41–7.35 (overlapping m, 4H, phenyl H), 7.24–7.09 (overlapping m, 3H, phenyl H), 7.03–6.78 (overlapping broad signal and m, 3H, phenyl H and N–H), 6.65 (broad signal, 1H, N–H) 3.29–3.22 (m, 6H, cationic N–CH₂), 1.62 (broad signal, 5H, B–H), 1.40 (t, *J* = 7.2 Hz, 9H, cationic N–CH₂CH₃), 1.22 (broad signal, 5H, B–H), 1.05 (broad signal, 1H, B–H). This spectrum contained small signals at 7.18, 6.71 and 6.67 ppm ascribed to residual aniline. ¹³C{¹H} NMR (100 MHz, CD₃CN, 23 °C): δ 165.6 (N=C–N), 138.1, 133.2, 131.3, 130.4, 130.1, 129.9, 127.5, 125.6 (8 aryl signals), 48.3 (cationic N–CH₂), 9.4 (cationic N–CH₃). This spectrum showed small signals at 149.1, 130.2, 118.3 and 115.6 ppm ascribed to residual aniline. ¹¹B{¹H} NMR (128 MHz, CD₂Cl₂, 23 °C): δ –5.8 (1B, B–N), –13.5 to –16.5 (10B, B–H), –17.4 (1B, B–H). High-resolution ESI-MS (negative mode, MeOH): *m/z* calcd for [C₁₃H₂₃B₁₂N₂][–]: 337.3056. Found: 337.2382.

Synthesis of amidine [Et₃NH](6c): A dry 20 mL vial, equipped with a stir bar, was charged with [Et₃NH]₂[B₁₂H₁₁NHCO₆H₃Cl₂] (177 mg, 0.33 mmol, 1 equiv). Then anhydrous MeCN (3 mL) was added, and dry Et₃N (0.45 mL, 3.25 mmol, 9.8 equiv) was added to the solution under N₂ protection. Pentafluorophenylcarboxylic acid chloride (128 mg, 0.55 mmol, 1.7 equiv) was added at 25 °C. The temperature was raised to 50 °C. After 30 min, *N,N*-dimethylethylamine (88 mg, 1.00 mmol, 3.0 equiv) was added. The mixture was stirred for another 4 h, and 1 M aqueous HCl (5 mL) was added. The suspension was extracted with EtOAc/MeCN 3:1 (5 × 10 mL). The combined organic layers were dried over MgSO₄, and the solution was filtered and concentrated by rotary evaporation. The cloudy residue was purified by silica gel column chromatography (eluent DCM/MeCN = 4:3, fraction size 20 mL). The combined eluates were concentrated and dried under vacuum at 60 °C overnight to afford compound [Et₃NH][6c] as a yellow solid (132 mg, 100%). ¹H{¹¹B} NMR (400 MHz, CD₃CN, 23 °C): δ 8.54 (broad signal, 1H, N–H), 7.59–7.55 (overlapping m, 3H, aryl H), 7.46 (broad signal, 1H, N–H), 6.98 (very broad signal, 1H, N–H), 3.43 (dt, *J* = 7.2 Hz, 7.2 Hz, 2H, CH₂), 3.24 (t, *J* = 7.2 Hz, 2H, CH₂), 2.77 (s, 6H, N–CH₃), 1.41 (broad signal, 5H, B–H), 1.12 (broad signal, 5H, B–H), 1.06 (broad signal, 1H, B–H). ¹³C{¹H} NMR (100 MHz, CD₃CN, 23 °C): δ 161.9 (N=C–N), 134.6, 134.2, 129.8, 129.2 (4 aryl signals), 56.9, 44.8, 40.0. ¹¹B{¹H} NMR (128 MHz, CD₃CN, 23 °C): δ –6.9 (1B, B–N), –13.0 to –18.0 (overlapping signals with peaks at –15.2 and –16.1 ppm, 11B, B–H). High-resolution ESI-MS (negative mode, MeOH): *m/z* calcd for [C₁₁H₂₇B₁₂Cl₂N₃–H][–]: 400.2699. Found: 400.2714.

Synthesis of urea [NBu₄]₂(7a): In a glovebox filled with N₂, a 20 mL vial was charged with [Et₃NH][B₁₂H₁₁NH₃] (260 mg, 1.00 mmol, 1 equiv), NaH (53 mg, 2.2 mmol, 2.2 equiv) and a stir bar. THF (10 mL) was added, and the mixture was stirred at room temperature for 10 min until there was no H₂ evolution anymore. Phenyl isocyanate (238 mg, 2.0 mmol, 2 equiv) was slowly added. The conversion was complete after stirring for 5 h. The flask was transferred out of the glovebox. The solvent was removed under vacuum, and H₂O (10 mL) was added. The aqueous solution was heated to 50 °C, and [NBu₄]Br (677 mg, 2.1 mmol, 2.1 equiv) was added. A white solid precipitated immediately and was collected by filtration. It was dried under vacuum overnight to afford [NBu₄]₂[7a] as a colorless microcrystalline product (685 mg, 90%). ¹H{¹¹B} NMR (400 MHz, CD₃CN): δ = 8.52 (broad s, 1H, anionic NH), 7.41 (d, 2H, *J* = 8.2 Hz, Ph H), 7.18 (dd, 2H, *J* = 8.2 Hz, 7.6 Hz, Ph–H), 6.83 (t, 1H, *J* = 7.6 Hz, Ph–H), 3.96 (broad s, 1H, NH), 3.25–3.01 (m, 16H, cationic N–CH₂), 1.67–1.50 (m, 16H, cationic N–CH₂CH₂), 1.41–1.27 (overlapping m and s, 21H, cationic N–CH₂CH₂CH₂ and B–H), 1.04 (s, 5H, B–H), 0.95 (t, 24H, *J* = 7.3 Hz, cationic CH₃), 0.85 (s, 1H, B–H). ¹³C{¹H} NMR (101 MHz, CD₃CN): δ = 158.6, 142.8, 129.5 (overlapping signals), 121.2, 59.2, 24.3, 20.3, 10.8. ¹¹B{¹H} NMR (128 MHz,

CD₃CN): $\delta = -5.0$ (1B, B–N), -15.4 (5B, B–H), -16.2 (5B, B–H), -19.3 (1B, B–H). High-resolution ESI-MS (negative mode, MeOH): m/z calcd for [C₇H₁₈B₁₂N₂O]²⁻ 138.1320. Found: 138.1331.

Synthesis of urea [PPh₄]₂(7b): This product was prepared in a similar manner to [NBu₄]₂[7a], using 4-chlorophenyl isocyanate (307 mg, 2.0 mmol, 2 equiv) and [PPh₄]Br (881 mg, 2.1 mmol, 2.1 equiv). [PPh₄]₂[7b] was obtained as a colorless microcrystalline solid (869 mg, 91%). ¹H{¹¹B} NMR (400 MHz, CD₃CN): $\delta = 8.59$ (s, 1H, anionic NH), 7.95–7.85 (m, 8H, cationic H), 7.81–5.58 (overlapping m, 32H, cationic H), 7.41–7.28 (m, 2H, Ph–H), 7.13–6.96 (m, 2H, Ph–H), 4.00 (s, 1H, N–H), 1.33 (broad signal, 5H, B–H), 1.07 (broad signal, 5H, B–H), 0.88 (broad signal, 1H, B–H). ¹³C{¹H} NMR (101 MHz, CD₃CN): $\delta = 158.4$, 141.7, 136.4 (d, $J_{PC} = 2.4$ Hz, cation CH), 135.6 (d, $J_{PC} = 10$ Hz, cation CH), 131.3 (d, $J_{PC} = 13.0$ Hz, cation CH), 129.2, 124.9, 119.6, 118.8 (d, $J_{PC} = 89$ Hz, cation C_q). ¹¹B{¹H} NMR (128 MHz, CD₃CN): $\delta = -5.0$ (1B, B–N), -15.5 (5B, B–H), -16.2 (5B, B–H), -19.2 (1B, B–H). High-resolution ESI-MS (negative mode, MeOH): m/z calcd for [C₇H₁₇B₁₂N₂OCl]²⁻ 155.1125. Found: 155.1133.

Synthesis of isocyanate [MePPh₃]₂(8): In a glovebox filled with N₂, a 50 mL round-bottom flask was charged with Cs[B₁₂H₁₁NH₃] (594 mg, 2.0 mmol, 1 equiv), NaH (144 mg, 6.0 mmol, 3 equiv) and a stir bar. DMF (10 mL) was added, and the mixture was stirred at 25 °C for 10 min until there was no H₂ evolution anymore. Then ClC(O)NMe₂ (6 equiv) diluted in DMF (2 mL) was slowly added by an Eppendorf pipet. The conversion was complete after stirring for 4 h. The flask was transferred out of the glovebox, and the volatiles were removed under vacuum. The residue was dissolved in H₂O (10 mL) at ca. 90 °C, giving a slightly yellow solution. The solution was stirred at 80–100 °C for 1 h, and [MePPh₃]Br (1.29 g, 5 mmol, 2.5 equiv) was added. A white precipitate formed, and it was collected by filtration. Purification by column chromatography (eluent DCM/MeCN 4:3) afforded [MePPh₃]₂[8] as a colorless solid (369 mg, 25%). ¹H{¹¹B} NMR (400 MHz, CD₃CN): $\delta = 7.90$ –7.83 (m, 6H, cationic CH), 7.76–7.62 (overlapping m, 24H, cationic CH), 2.83 (d, $J = 13.8$ Hz, 6H, CH₃), 1.23 (broad signal, 5H, B–H), 0.97 (broad signal, 5H, B–H), 0.75 (broad signal, 1H, B–H). ¹³C{¹H} NMR (101 MHz, CD₃CN): $\delta = 136.1$ (d, $J_{PC} = 3.0$ Hz, cation CH), 134.2 (d, $J_{PC} = 11$ Hz, cation CH), 131.1 (d, $J_{PC} = 13$ Hz, cation CH), 120.4 (d, $J_{PC} = 89$ Hz, cation C_q), 9.37 (d, $J_{PC} = 58$ Hz, cation CH₃). The N=C=O carbon atom could not be detected unambiguously. ¹¹B{¹H} NMR (128 MHz, CD₃CN): $\delta = -7.74$ (1B, B–N), -15.4 (5B, B–H), -16.7 (5B, B–H), -19.6 (1B, B–H). Mass-spectrometric characterization of this product proved difficult; the results that were obtained by negative-mode ESI-MS are shown in Figure S2, along with the IR spectrum in Figure S3.

Additional figures, X-ray crystallographic data and copies of NMR spectra are provided in the Supporting Information file; see “Supplementary Materials”.

4. Conclusions

In summary, the synthesis and characterization of a series of compounds based on the amino-dodecaborate anion **2** has been achieved, including amidinium ions **6**, amides **3**, ureas **7** and dodecaboranyl isocyanate **8**. The new products have been fully characterized spectroscopically, and solid-state structures have been elucidated for nine derivatives. Amidinium ions **7** are reported for the first time, as well as aromatic ureas of the structure {B₁₂}NH-C(O)-NHAr. A facile method for the interconversion of the dianionic and monoanionic form of amides **3** has been developed, which is of relevance in view their different physical properties, in particular solubility and crystallinity. A fragmentation-based approach to dodecaboranyl isocyanate **8** was developed, which is expected to provide access to novel {B₁₂} derivatives by subsequent nucleophilic addition to the NCO group or by pericyclic reactions. The transformations leading to **6**, **7** and **8** extend the synthetic toolbox to produce boron clusters for applications in various areas.

Supplementary Materials: The following are available online: Supporting Information file with experimental procedures and spectroscopic data. Crystal structures have been deposited with the Cambridge Crystallographic Data Centre: CCDC1861483–1861492. They are available free of charge from www.ccdc.cam.ac.uk.

Author Contributions: Y.Z. and Y.S. carried out the majority of the synthetic work and contributed equally; T.W. conducted additional experiments; J.L. and B.S. solved the X-ray crystal structures; Y.Z. and S.D. wrote the manuscript; S.D. supervised the study.

Funding: This research was funded by the Natural Science Foundation of China (grant no. 21472166), the National Basic Research Program of China (973 project 2015CB856500) and the Chinese “1000 Young Talents Plan”.

Conflicts of Interest: The authors declare no conflict of interest.

References

1. Hosmane, N.S. *Boron Science: New Technologies and Applications*, 1st ed.; CRC Press, Taylor & Francis Group: Boca Raton, FL, USA, 2012.
2. Sivaev, I.B.; Bregadze, V.I.; Sjöberg, S. Chemistry of closo-dodecaborate anion $[B_{12}H_{12}]^{2-}$: A Review. *Collect. Czech. Chem. Commun.* **2002**, *67*, 679–727. [[CrossRef](#)] [[PubMed](#)]
3. Axtell, J.C.; Saleh, L.M.A.; Qian, E.A.; Wixtrom, A.I.; Spokoiny, A.M. Synthesis and Applications of Perfunctionalized Boron Clusters. *Inorg. Chem.* **2018**, *57*, 2333–2350. [[CrossRef](#)] [[PubMed](#)]
4. Poater, J.; Solà, M.; Viñas, C.; Teixidor, F. Hückel’s Rule of Aromaticity Categorizes Aromatic closo Boron Hydride Clusters. *Chem. Eur. J.* **2016**, *22*, 7437–7443. [[CrossRef](#)] [[PubMed](#)]
5. Knapp, C. Weakly coordinating anions: halogenated borates and dodecaborates. In *Comprehensive Inorganic Chemistry II*; Elsevier: Amsterdam, The Netherlands, 2013; pp. 651–679.
6. Bolli, C.; Derendorf, J.; Jenne, C.; Scherer, H.; Sindlinger, C.P.; Wegener, B. Synthesis and Properties of the Weakly Coordinating Anion $[Me_3NB_{12}Cl_{11}]^-$. *Chem. Eur. J.* **2014**, *20*, 13783–13792. [[CrossRef](#)] [[PubMed](#)]
7. Kessler, M.; Knapp, C.; Sagawe, V.; Scherer, H.; Uzun, R. Synthesis, Characterization, and Crystal Structures of Silylium Compounds of the Weakly Coordinating Dianion $[B_{12}Cl_{12}]^{2-}$. *Inorg. Chem.* **2010**, *49*, 5223–5230. [[CrossRef](#)] [[PubMed](#)]
8. Bolli, C.; Derendorf, J.; Keßler, M.; Knapp, C.; Scherer, H.; Schulz, C.; Warneke, J. Synthesis, Crystal Structure, and Reactivity of the Strong Methylating Agent $Me_2B_{12}Cl_{12}$. *Angew. Chem. Int. Ed.* **2010**, *49*, 3536–3538. [[CrossRef](#)] [[PubMed](#)]
9. Avelar, A.; Tham, F.S.; Reed, C.A. Superacidity of Boron Acids $H_2(B_{12}X_{12})$ ($X=Cl, Br$). *Angew. Chem. Int. Ed.* **2009**, *48*, 3491–3493. [[CrossRef](#)] [[PubMed](#)]
10. Geis, V.; Guttsche, K.; Knapp, C.; Scherer, H.; Uzun, R. Synthesis and characterization of synthetically useful salts of the weakly-coordinating dianion $[B_{12}Cl_{12}]^{2-}$. *Dalton Trans.* **2009**, 2687–2694. [[CrossRef](#)] [[PubMed](#)]
11. Peryshkov, D.V.; Strauss, S.H. Exceptional Structural Compliance of the $B_{12}F_{12}^{2-}$ Superweak Anion. *Inorg. Chem.* **2017**, *56*, 4072–4083. [[CrossRef](#)] [[PubMed](#)]
12. Malischewski, M.; Peryshkov, D.V.; Bukovsky, E.V.; Seppelt, K.; Strauss, S.H. Structures of $M_2(SO_2)_6B_{12}F_{12}$ ($M = Ag$ or K) and $Ag_2(H_2O)_4B_{12}F_{12}$: Comparison of the Coordination of SO_2 versus H_2O and of $B_{12}F_{12}^{2-}$ versus Other Weakly Coordinating Anions to Metal Ions in the Solid State. *Inorg. Chem.* **2016**, *55*, 12254–12262. [[CrossRef](#)] [[PubMed](#)]
13. Ivanov, S.V.; Miller, S.M.; Anderson, O.P.; Solntsev, K.A.; Strauss, S.H. Synthesis and Stability of Reactive Salts of Dodecafluoro-closo-dodecaborate(2−). *J. Am. Chem. Soc.* **2003**, *125*, 4694–4695. [[CrossRef](#)] [[PubMed](#)]
14. Ivanov, S.V.; Davis, J.A.; Miller, S.M.; Anderson, O.P.; Strauss, S.H. Synthesis and Characterization of Ammonioundecafluoro-closo-dodecaborates(1−). New Superweak Anions. *Inorg. Chem.* **2003**, *42*, 4489–4491. [[CrossRef](#)] [[PubMed](#)]
15. Leśnikowski, Z.J. Challenges and Opportunities for the Application of Boron Clusters in Drug Design. *J. Med. Chem.* **2016**, *59*, 7738–7758. [[CrossRef](#)] [[PubMed](#)]
16. Gabel, D. Boron clusters in medicinal chemistry: perspectives and problems. *Pure Appl. Chem.* **2015**, *87*, 173–179. [[CrossRef](#)]
17. Scholz, M.; Hey-Hawkins, E. Carbaboranes as Pharmacophores: Properties, Synthesis, and Application Strategies. *Chem. Rev.* **2011**, *111*, 7035–7062. [[CrossRef](#)] [[PubMed](#)]
18. Wegener, M.; Huber, F.; Bolli, C.; Jenne, C.; Kirsch, S.F. Silver-Free Activation of Ligated Gold(I) Chlorides: The Use of $[Me_3NB_{12}Cl_{11}]^-$ as a Weakly Coordinating Anion in Homogeneous Gold Catalysis. *Chem. Eur. J.* **2015**, *21*, 1328–1336. [[CrossRef](#)] [[PubMed](#)]

19. Messina, M.S.; Axtel, J.C.; Wang, Y.; Chong, P.; Wixtrom, A.I.; Kirlikovali, K.O.; Upton, B.M.; Hunter, B.M.; Shafaat, O.S.; Khan, S.I.; et al. Visible-Light-Induced Olefin Activation Using 3D Aromatic Boron-Rich Cluster Photooxidants. *J. Am. Chem. Soc.* **2016**, *138*, 6952–6955. [[CrossRef](#)] [[PubMed](#)]
20. Zhang, Y.; Liu, J.; Duttwyler, S. Synthesis and Structural Characterization of Ammonio/Hydroxo Undecachloro-*closo*-dodecaborates $[B_{12}Cl_{11}(NH_3)]^- / [B_{12}Cl_{11}(OH)]^{2-}$ and Their Derivatives. *Eur. J. Inorg. Chem.* **2015**, 5158–5162. [[CrossRef](#)]
21. Kirchmann, M.; Wesemann, L. Amino-*closo*-dodecaborate—A new ligand in coordination chemistry. *Dalton Trans.* **2008**. [[CrossRef](#)] [[PubMed](#)]
22. Kirchmann, M.; Wesemann, L. η^1 and η^2 Coordination of 1-amino-*closo*-dodecaborate. *Dalton Trans.* **2008**. [[CrossRef](#)] [[PubMed](#)]
23. Warneke, J.; Jenne, C.; Bernarding, J.; Azov, V.A.; Plaumann, M. Evidence for an intrinsic binding force between dodecaborate dianions and receptors with hydrophobic binding pockets. *Chem. Commun.* **2016**, *52*, 6300–6303. [[CrossRef](#)] [[PubMed](#)]
24. Assaf, K.I.; Gabel, D.; Zimmermann, W.; Nau, W.M. High-affinity host-guest chemistry of large-ring cyclodextrins. *Org. Biomol. Chem.* **2016**, *14*, 7702–7706. [[CrossRef](#)] [[PubMed](#)]
25. Wang, W.; Wang, X.; Cao, J.; Liu, J.; Qi, B.; Zhou, X.; Zhang, S.; Gabel, D.; Nau, W.M.; Assaf, K.I.; et al. The chaotropic effect as an orthogonal assembly motif for multi-responsive dodecaborate-cucurbituril supramolecular networks. *Chem. Commun.* **2018**, *54*, 2098–2101. [[CrossRef](#)] [[PubMed](#)]
26. Assaf, K.I.; Suckova, O.; Danaf, N.A.; von Glasenapp, V.; Gabel, D.; Nau, W.M. Dodecaborate-Functionalized Anchor Dyes for Cyclodextrin-Based Indicator Displacement Applications. *Org. Lett.* **2016**, *18*, 932–935. [[CrossRef](#)] [[PubMed](#)]
27. Assaf, K.I.; Ural, M.S.; Pan, F.; Georgiev, T.; Simova, S.; Rissanen, K.; Gabel, D.; Nau, W.M. Water Structure Recovery in Chaotropic Anion Recognition: High-Affinity Binding of Dodecaborate Clusters to γ -Cyclodextrin. *Angew. Chem. Int. Ed.* **2015**, *54*, 6852–6856. [[CrossRef](#)] [[PubMed](#)]
28. Pitochelli, A.R.; Hawthorne, F.M. The isolation of the icosahedral $B_{12}H_{12}^{2-}$ Ion. *J. Am. Chem. Soc.* **1960**, *82*, 3228–3229. [[CrossRef](#)]
29. Olid, D.; Núñez, R.; Viñas, C.; Teixidor, F. Methods to produce B–C, B–P, B–N and B–S bonds in boron clusters. *Chem. Soc. Rev.* **2013**, *42*, 3318–3336. [[CrossRef](#)] [[PubMed](#)]
30. Grüner, B.; Bonnetot, B.; Mongeot, H. Synthesis of N- and B-substituted derivatives of *closo*-amino-undecahydro-dodecaborate(1[−]) anion. *Collect. Czech. Chem. Commun.* **1997**, *62*, 1185–1204. [[CrossRef](#)]
31. Hertler, W.R.; Raasch, M.S. Chemistry of boranes. XIV. Amination of $B_{10}H_{10}^{2-}$ and $B_{12}H_{12}^{2-}$ with hydroxylamine-*O*-sulfonic acid. *J. Am. Chem. Soc.* **1964**, *86*, 3661–3668. [[CrossRef](#)]
32. Dudenkov, I.V.; Zhizhin, K.Yu.; Chernyavskii, A.S.; Katser, S.B.; Goeva, L.V.; Sergienko, V.S.; Solntsev, K.A.; Kuznetsov, N.T. Synthesis and Crystal Structure of 1,7-(NH_3)₂ $B_{12}H_{10} \cdot 0.5 H_2O$. *Russ. J. Inorg. Chem.* **2000**, *45*, 1864–1867.
33. Genady, A.R.; El-Zaria, M.E.; Gabel, D. Non-covalent assemblies of negatively charged boronated porphyrins with different cationic moieties. *J. Organomet. Chem.* **2004**, *689*, 3242–3250. [[CrossRef](#)]
34. Hoffmann, S.; Justus, E.; Ratajski, M.; Lork, E.; Gabel, D. $B_{12}H_{11}$ -containing guanidinium derivatives by reaction of carbodiimides with $H_3N-B_{12}H_{11}(1^-)$. A new method for connecting boron clusters to organic compounds. *J. Organomet. Chem.* **2005**, *690*, 2757–2760. [[CrossRef](#)]
35. Koo, M.-S.; Ozawa, T.; Santos, R.A.; Lamborn, K.R.; Bollen, A.W.; Deen, D.F.; Kahl, S.B. Synthesis and Comparative Toxicology of a Series of Polyhedral Borane Anion-Substituted Tetraphenyl Porphyrins. *J. Med. Chem.* **2007**, *50*, 820–827. [[CrossRef](#)] [[PubMed](#)]
36. El-Zaria, M.E.; Ban, H.S.; Nakamura, H. Boron-Containing Protoporphyrin IX Derivatives and Their Modification for boron Neutron Capture Therapy: Synthesis, Characterization, and Comparative In Vitro Toxicity Evaluation. *Chem. Eur. J.* **2010**, *16*, 1543–1552. [[CrossRef](#)] [[PubMed](#)]
37. Sun, Y.; Zhang, J.; Zhang, Y.; Liu, J.; van der Veen, S.; Duttwyler, S. The *closo*-Dodecaborate Dianion Fused with Oxazoles Provides 3D Diboraheterocycles with Selective Antimicrobial Activity. *Chem. Eur. J.* **2018**, *24*, 10364–10371. [[CrossRef](#)] [[PubMed](#)]

38. Sivaev, I.B.; Bruskin, A.B.; Nesterov, V.V.; Antipin, M.Y.; Bregadze, V.I.; Sjöberg, S.S. Synthesis of Schiff Bases Derived from the Ammoniaundecahydro-*closo*-dodecaborate (1−) Anion, $[B_{12}H_{11}NH=CHR]^-$, and Their Reduction into Monosubstituted Amines $[B_{12}H_{11}NH_2CH_2R]^-$: A New Route to Water Soluble Agents for BNCT. *Inorg. Chem.* **1999**, *38*, 5887–5893. [[CrossRef](#)]
39. Zhang, Y.; Sun, Y.; Lin, F.; Liu, J.; Duttwyler, S. Rhodium (III)-Catalyzed Alkenylation–Annulation of *closo*-Dodecaborate Anions through Double B–H Activation at Room Temperature. *Angew. Chem. Int. Ed.* **2016**, *50*, 15609–15614. [[CrossRef](#)] [[PubMed](#)]
40. Alam, F.; Soloway, A.H.; Barth, R.F.; Mafune, N.; Adams, D.M.; Knoth, W.H. Boron Neutron Capture Therapy: Linkage of a Boronated Macromolecule to Monoclonal Antibodies Directed Against Tumor-Associated Antigens. *J. Med. Chem.* **1989**, *32*, 2326–2330. [[CrossRef](#)] [[PubMed](#)]
41. Ozaki, S. Recent Advances in Isocyanate Chemistry. *Chem. Rev.* **1972**, *72*, 457–496. [[CrossRef](#)]
42. Nyquist, R.A. *Interpreting Infrared, Raman, and Nuclear Magnetic Resonance Spectra*, 1st ed.; Academic Press: Cambridge, MA, USA, 2001; p. 46.

Sample Availability: Not available.



© 2018 by the authors. Licensee MDPI, Basel, Switzerland. This article is an open access article distributed under the terms and conditions of the Creative Commons Attribution (CC BY) license (<http://creativecommons.org/licenses/by/4.0/>).